Research Paper
Computational Methods for Differential Equations
http://cmde.tabrizu.ac.ir
Vol. 12, No. 3, 2024, pp. 454-470
DOI:10.22034/cmde.2023.56465.2359

Efficiency of vaccines for COVID-19 and stability analysis with fractional derivative

Mohammad Esmael Samei[1,*], Lotfollah Karimi[2], Mohammed K. A. Kaabar[3,4], Roya Raeisi[5], Jehad Alzabut[6,7], and Francisco Martínez González[8]

[1]Department of Mathematics, Faulty of Basic Science, Bu-Ali Sina University, Hamedan 65178-38695, Iran.

[2]Department of Mathematics, Hamedan University of Technology, Hamedan, Iran.

[3]Gofa Camp, Near Gofa Industrial College and German Adebabay, Nifas Silk-Lafto, 26649 Addis Ababa, Ethiopia.

[4]Institute of Mathematical Sciences, Faculty of Science, University of Malaya, Kuala Lumpur 50603, Malaysia.

[5]Department of Pediatrics, Hamadan University of Medical Science, Hamadan, Iran.

[6]Department of Mathematics and General Sciences, Prince Sultan University, Riyadh, Saudi Arabia.

[7]Department of Industrial Engineering, OSTİM Technical University, 06374 Ankara, Turkey.

[8]Department of Applied Mathematics and Statistics, Technological University of Cartagena, Cartagena 30203, Spain.

Abstract

The objectives of this study are to develop the SEIR model for COVID-19 and evaluate its main parameters such as therapeutic vaccines, vaccination rate, and effectiveness of prophylactic. Global and local stability of the model and numerical simulation are examined. The local stability of equilibrium points was classified. A Lyapunov function is constructed to analyze the global stability of the disease-free equilibrium. The simulation part is based on two situations, including the USA and Iran. Our results provide a good contribution to the current research on this topic.

Keywords. Efficiency of vaccines, Numerical simulation, Equilibrium point, COVID-19.

2010 Mathematics Subject Classification. 34A08, 65P99, 49J15.

1. Introduction

The ponder of illness flow may be an overwhelming subject for numerous scientists and mathematicians. Any condition which interferes with the normal functioning of the body and causes discomfort, disability, or impairment of the health of a living organism is called a disease. The impact of severe diseases on people is a real concern in terms of suffering as well as social and economic implications. The control of these acute diseases has been a great concern for bio-mathematicians and medical experts. It has been approved that these infectious diseases are fatal to billions of people and can also cause the loss of their worth. Mathematical modeling plays a crucial role in the study of these adverse types of diseases [1, 4, 20, 23, 28, 30].

In the recent era, Corona virus 2 is the cause of COVID-19 which is a severe acute respiratory disease [1, 27, 31]. Golmankhaneh *el al.* formulated fractal functional differential equations as a framework that provides a mathematical model for the phenomena with fractal time and fractal structure [11]. The droplets, airborne, and closed contact transmission lead to virus spread from person to person [2, 5, 12, 14]. Symptoms of many COVID-19 infected patients are minimal [13, 16, 21]. Recent reports indicate that $15-45\%$ of COVID-19 cases are asymptomatic, which includes two categories:

- Asymptomatic (meaning those who never become symptomatic),
- Pre-symptomatic (pre-symptomatic means asymptomatic people who subsequently become symptomatic).

Received: 06 May 2023 ; Accepted: 09 October 2023.
∗ Corresponding author. Email: mesamei@basu.ac.ir.

Symptoms of COVID-19 patients were mild, moderate, and severe. They included joint pain, cough, nasal congestion, diarrhea, runny nose, fatigue, chills, headache, muscle pain, nausea, sore throat, vomiting, and fever. The first known human coronavirus infection occurred in early December 2019. The virus first broke out in mid-December 2019 in Wuhan, China, and in a short period caused many casualties [31]. Nowadays, the virus has recently caused epidemics around the world in more than 215 countries with 35,604,464 confirmed cases and 1,120,378 mortality, as of October 2, 2021. https://covid19.who.int. Due to the extent of the damage that COVID-19 has done to the world, various research is underway to find the best way to reduce the spread of COVID-19, but until this research, no definitive treatment has been found [15, 19]. By increasing of COVID-19 cases, predicting the number of infected cases and the termination of COVID-19 are important. Despite the production of effective vaccines against COVID-19, unfortunately, countries with limited resources, such as Iran, have not yet been able to bring their vaccination coverage to an acceptable level, and this is due to the injustice of the economic system worldwide [1]. Therefore, in these circumstances, it seems that mathematical models predict the spread of disease, especially for health policymakers in these countries to adopt the necessary policies to control the disease and prevent its spread. The infectious disease mathematical model is a crucial tool that has been used to study the spreading mechanism of diseases [1].

In this research, we created the well-known frame of the SEIR model with four compartments of

- Susceptible population, (S);
- Exposed population, (E);
- Infectious population, (I);
- Recovered population, (R);

to investigate a system of ordinary differential equations to model the efficiency of vaccines for the COVID-19 situation in the US and Iran. In this model, we divide people into four groups which is the dynamics diagram of the COVID-19 disease model shown in Figure 1. The SEIR model is appropriate for malady transmission in which a contaminated

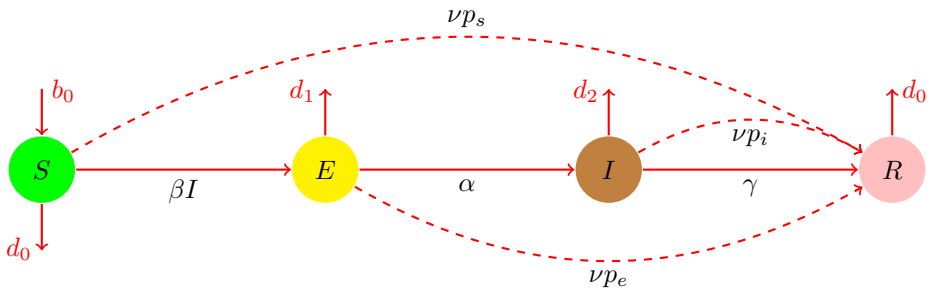

FIGURE 1. Model SEIR for COVID-19.

person needs a brief period to be irresistible. In this study, we employed the SEIR prepared with the adequacy of immunization to figure the COVID-19 circumstance when an antibody comes out.

In 2020, Rezapour *et al.* provided a SEIR epidemic model (Figure 2)

$$\begin{cases} \dfrac{\mathrm{dS}}{\mathrm{dt}} = \omega\mu\mathtt{S} - (\beta_1\mathtt{E} + \beta_2\mathtt{I})\mathtt{S}, \\ \dfrac{\mathrm{dE}}{\mathrm{dt}} = (\beta_1\mathtt{E} + \beta_2\mathtt{I})\mathtt{S} - (\lambda + \mu)\mathtt{E}, \\ \dfrac{\mathrm{dI}}{\mathrm{dt}} = \lambda\mathtt{E} - (\tau + \mu + \delta)\mathtt{I}, \\ \dfrac{\mathrm{dR}}{\mathrm{dt}} = \tau\mathtt{I} - \mu\mathtt{R}, \end{cases}$$

for the spread of COVID-19 using the Caputo fractional derivative where $\omega = n \times N$, N is the total number of individuals and n is the birth rate, μ is the death rate of people, β_1, β_2 are the transmission rate of infection from $\mathtt{E}$ to $\mathtt{S}$, $\mathtt{I}$ to $\mathtt{S}$, respectively, λ is the transmission rate of people from $\mathtt{E}$ to $\mathtt{I}$, δ is the mortality rate due to the disease, and τ is the rate of recovery of infected people [24]. Also, the feasibility region of the system and its equilibrium points were calculated, and the stability of the equilibrium points and the approximate solution to the model were investigated via fixed point theory and fractional Euler method [24]. To predict the transmission of COVID-19 in Iran and in the world, we provide a numerical simulation based on real data [24].

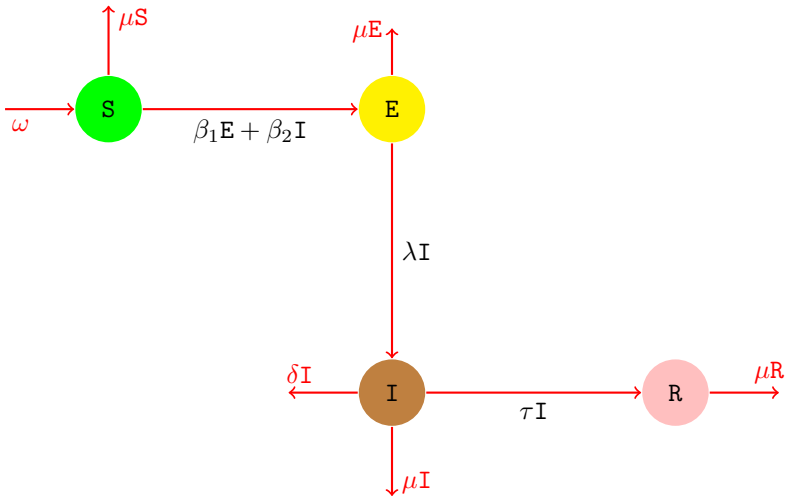

FIGURE 2. SEIR model of COVID-19 introduce by authors in [24].

Khan *et al.* in [3], described the mathematical modeling and dynamics of a novel corona virus (2019-nCoV)

$$\begin{cases} \dfrac{d\mathtt{S}_b}{dt} = \omega\Pi_b - \mu_b\mathtt{S}_b - \dfrac{\eta_b\mathtt{S}_b\mathtt{I}_b}{\mathtt{N}_b}, \\ \dfrac{d\mathtt{E}_b}{dt} = \dfrac{\eta_b\mathtt{S}_b\mathtt{I}_b}{\mathtt{N}_b} - (\mu_b + \theta_b)\mathtt{E}_b, \\ \dfrac{d\mathtt{I}_b}{dt} = \theta_b\mathtt{E}_b - (\tau_b + \mu_b)\mathtt{I}_b, \\ \dfrac{d\mathtt{R}_b}{dt} = \tau_b\mathtt{I}_b - \mu_b\mathtt{R}_b, \end{cases} \qquad \begin{cases} \dfrac{d\mathtt{S}_h}{dt} = \omega\Pi_h - \mu_h\mathtt{S}_h - \dfrac{\eta_{bh}\mathtt{S}_h\mathtt{I}_b}{\mathtt{N}_h} - \dfrac{\eta_h\mathtt{S}_h\mathtt{I}_h}{\mathtt{N}_h}, \\ \dfrac{d\mathtt{E}_h}{dt} = \dfrac{\eta_{bh}\mathtt{S}_h\mathtt{I}_b}{\mathtt{N}_h} + \dfrac{\eta_h\mathtt{S}_h\mathtt{I}_h}{\mathtt{N}_h} - (\mu_h + \theta_h)\mathtt{E}_h, \\ \dfrac{d\mathtt{I}_h}{dt} = \theta_h\mathtt{E}_h - (\tau_h + \mu_h)\mathtt{I}_h, \\ \dfrac{d\mathtt{R}_h}{dt} = \tau_h\mathtt{I}_h - \mu_h\mathtt{R}_h, \end{cases}$$

by reducing the model with the assumptions that the seafood market has enough sources of infection and then formulate a fractional model where $\mathtt{S}_b(t)$, $\mathtt{E}_b(t)$, $\mathtt{I}_b(t)$, and $\mathtt{R}_b(t)$ at any time t with $\mathtt{N}_b(t) = \mathtt{S}_b(t) + \mathtt{E}_b(t) + \mathtt{I}_b(t) + \mathtt{R}_b(t)$, and $\mathtt{N}_h(t)$ is unknown host, which is classified into four subgroups, that is $\mathtt{S}_h(t)$, $\mathtt{E}_h(t)$, $\mathtt{I}_h(t)$, and $\mathtt{R}_h(t)$ respectively, show the susceptible, exposed, infected and the recovered or removed hosts with

$$\mathtt{N}_h(t) = \mathtt{S}_h(t) + \mathtt{E}_h(t) + \mathtt{I}_h(t) + \mathtt{R}_h(t).$$

Figure 3 shows the model. In 2021, Qesmi *et al.* introduced models of increasing complexity for COVID-19 trans-

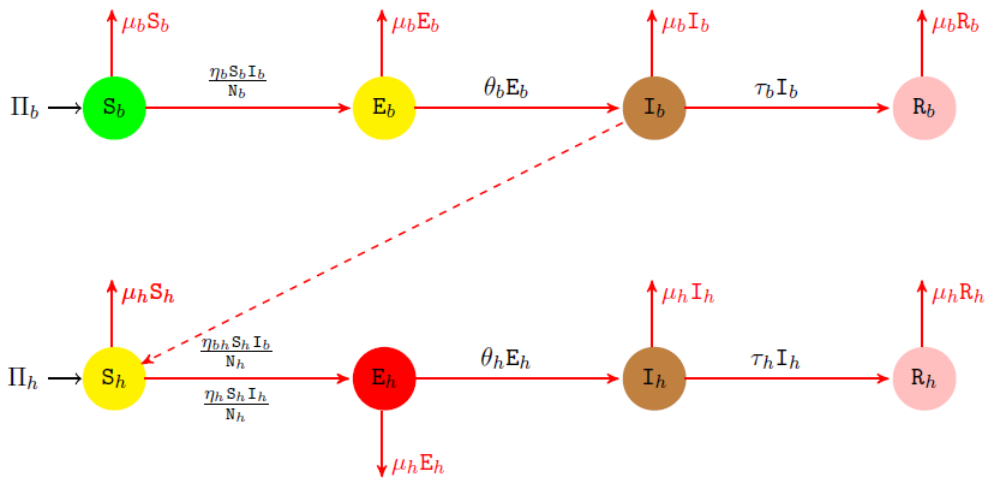

FIGURE 3. Interaction among basts and host in [3].

mission by considering an SEAIR model

$$\begin{cases} \frac{dS}{dt} = -((1-\gamma)p\beta_c + (1-\theta)(1-(1-\gamma)p)\beta_N)S(t)(A(t)+S_u(t)/N, \\ \frac{dE}{dt} = ((1-\gamma)p\beta_c + (1-\theta)(1-(1-\gamma)p)\beta_N)S(t)(A(t)+I_u(t))/N - k\,E, \\ \frac{dA}{dt} = kE - \delta A(t), \quad \frac{dI_u}{dt} = \delta_1 A(t) - \mu I_u(t) - dI_u(t), \\ \frac{dH}{dt} = \delta_2 A(t) - \mu H - dH, \quad \frac{dR}{dt} = \mu(H + I_u(t)), \quad \frac{dD}{dt} = d(H + I_u(t)), \end{cases}$$

including basic characteristics related to COVID-19 [22]. In addition, Baba *et al.* constructed a fractional order COVID-19 model SEIHRV consisting of six compartments in Caputo sense

$$\begin{cases} {}_0^C D_t^\alpha S(t) = Y^\alpha - \beta^\alpha SI - \theta^\alpha SV - \mu^\alpha S, \\ {}_0^C D_t^\alpha E(t) = \beta^\alpha SI + \theta^\alpha SV - (\mu^\alpha + \gamma^a lpha + \eta_1^\alpha)\,E, \\ {}_0^C D_t^\alpha I(t) = \gamma^\alpha E - (\mu^\alpha + \pi^\alpha + \zeta_1^\alpha + \eta_2^\alpha)\,I, \\ {}_0^C D_t^\alpha H(t) = \pi^\alpha I - (\mu^\alpha + \zeta_2^\alpha + \eta_3^\alpha)\,H, \\ {}_0^C D_t^\alpha R(t) = \eta_1^\alpha E + \eta_2^\alpha I + \eta_3^\alpha H - \mu^\alpha R, \\ {}_0^C D_t^\alpha V(t) = q_1^\alpha E + q_2^\alpha I - r^\alpha R, \end{cases}$$

where the compartments $S(t)$, $E(t)$, $I(t)$, $H(t)$, $R(t)$, and $V(t)$ stands for susceptible, exposed, infected, hospitalized, recovered, and virus compartments, respectively, to study the shedding effect, by adding compartment $V(t)$ for contaminated surfaces [6].

The future situation of an outbreak can be predicted by a mathematical model. It can also assess the leading technique to control spreading illnesses. There are numerous distinctive sorts of numerical models for foreseeing a plague disease. One of them is called compartment models. A compartment demonstrates a curious apparatus for the COVID-19 circumstance. A recent research study has been conducted on studying the model related to the efficiency

of vaccines for COVID-19 situation in US and India [29].

The rest of this paper is arranged as follows: In section 2, we remember what fractional integral and derivative mean. We make a plan and look at all the places where things balance out. Then we see if these places are stable both in the whole world and in their smaller surroundings. This is explained in section 3. Section 4 is where we find solutions that are greater than or equal to zero for model 3.1. We try out model 3.1 in two situations. Specifically, we use measurements from the USA and Iran that we wrote down in section 5. We looked at the situation in both countries and made a guess about how bad COVID-19 could get once vaccines are available. This is explained in section 5. In section 6, there is a conclusion about the model 3.1.

2. Preliminaries

This section is dedicated to introduce some introductory definitions and the fundamental concepts of fractional differential calculus (some related studies can be seen in [17, 25]). Recently, a new definition of fractional derivative and fractional integration has hugely evolved, namely the derivatives with nonsingular kernel and new Riemann-Liouville fractional derivative without singular kernel to the two-parameter derivatives with non-singular and nonlocal kernel [7, 9, 10].

Among all these, the two most commonly used definitions are defined as follows: The Rieman-Liouville and Caputo ($C\mathbb{FD}$) derivative of order λ for an integrable function φ, are defined as form

$$\mathscr{D}_{\mathfrak{t}}^{\lambda}\varphi(\mathfrak{t}) = \begin{cases} \dfrac{1}{\Gamma(\mathrm{m}-\lambda)}\dfrac{\mathrm{d}^{\mathrm{m}}}{\mathrm{d}\mathfrak{t}^{\mathrm{m}}}\displaystyle\int_0^{\mathfrak{t}} \frac{\varphi(\xi)}{(\mathfrak{t}-\xi)^{\lambda-\mathrm{m}+1}}\,\mathrm{d}\xi, & \mathrm{m}-1<\lambda<\mathrm{m}, \\ \dfrac{\mathrm{d}^{\mathrm{m}}}{\mathrm{d}\mathfrak{t}^{\mathrm{m}}}\varphi(\mathfrak{t}), & \lambda=\mathrm{m}\in\mathbb{N}, \end{cases} \tag{2.1}$$

and

$$\mathscr{D}_{*}^{\lambda}\varphi(\mathfrak{t}) = \begin{cases} \dfrac{1}{\Gamma(\mathrm{m}-\lambda)}\displaystyle\int_0^{\mathfrak{t}} \frac{\varphi^{(\mathrm{m})}(\xi)}{(\mathfrak{t}-\xi)^{\lambda-\mathrm{m}+1}}\,\mathrm{d}\xi, & 0\le \mathrm{m}-1<\lambda<\mathrm{m},\ \mathrm{m}\in\mathbb{N}, \\ \dfrac{\mathrm{d}^{\mathrm{m}}}{d\mathfrak{t}^{\mathrm{m}}}\varphi(\mathfrak{t}), & \lambda=\mathrm{m},\ \mathrm{m}\in\mathbb{N}. \end{cases} \tag{2.2}$$

respectively. The most used definition of the Riemann-Liouville fractional integration is given by

$$\mathscr{I}^{\lambda}\varphi(\mathfrak{t}) = \begin{cases} \dfrac{1}{\Gamma(\lambda)}\displaystyle\int_0^{\mathfrak{t}} \frac{\varphi(\xi)}{(\mathfrak{t}-\xi)^{-\lambda+1}}\,\mathrm{d}\xi, & \mathfrak{t}>0, \lambda>0, \\ \varphi(\mathfrak{t}), & \lambda=0. \end{cases} \tag{2.3}$$

The relation between Caputo fractional differential operator and Riemann-Liouville integral operator is given by the following.

Lemma 2.1. *[18] Let m be a positive integer number and $\mathrm{m}-1<\lambda\le \mathrm{m}$ then $\mathscr{D}_{*}^{\lambda}\mathscr{I}^{\lambda}\varphi(\mathfrak{t})=\varphi(\mathfrak{t})$ and*

$$\mathscr{I}^{\lambda}\mathscr{D}_{*}^{\lambda}\varphi(\mathfrak{t}) = \varphi(\mathfrak{t}) - \sum_{\varkappa=0}^{\mathrm{m}-1}\varphi^{(\varkappa)}(0)\frac{\mathfrak{t}^{\varkappa}}{\varkappa!}, \qquad \mathfrak{t}>0.$$

We use this lemma in most of Theorems in this paper.

3. Creating a plan or strategy to solve a problem

In viral pandemic, mathematical models are important for predicting virus behavior and how it is transmitted from person to person in different parts of the world to help manage the disease. To evaluate the prevalence of diseases, various mathematical models such as `SIR`, `SIRD`, `SEIRD`, `SIRS`, `SEAIHRD`, `MSEIR`, `SIRC`, `SEIR`, etc. are used. According to the World Health Organization, there are two types of people with COVID-19. The timelines of infection within the host can be best described with reference to the dynamics of infectiousness and of disease (Figure 4). Both start

with the active disease of the vulnerable host by the parasite. The timeline of infectiousness includes the latent period, the time interval from infection to development of infectiousness, and the period of infectiousness of the host, during which time the host could infect another host.

Eventually, the host becomes noninfectious either by recovery from the infection, possibly developing immunity, or by death. The host can also become noninfectious while still alive and still harboring the parasite [1]. The timeline of disease within the host includes the incubation period, the time from infection to development of symptomatic disease, and the symptomatic period. The probability of developing symptoms or disease after becoming infected is the pathogenicity of the interaction of the parasite with the host. Eventually, the host leaves the symptomatic state either by recovering from the symptoms or by death. The host becomes an infectious carrier if he recovers from symptoms but remains infectious. The terminology used in infectious disease epidemiology always differs from that of non-infectious disease epidemiology. The term latent period refers the time corresponding to the period from the development of asymptomatic disease to the development of symptoms. The incubation period in infectious disease is a combination of what is called the induction and the latent periods in noninfectious diseases. The way two lines on Figure 4 are set up and how they are connected is different for each parasite. This can affect the health of lots of people and how studies are designed [1].

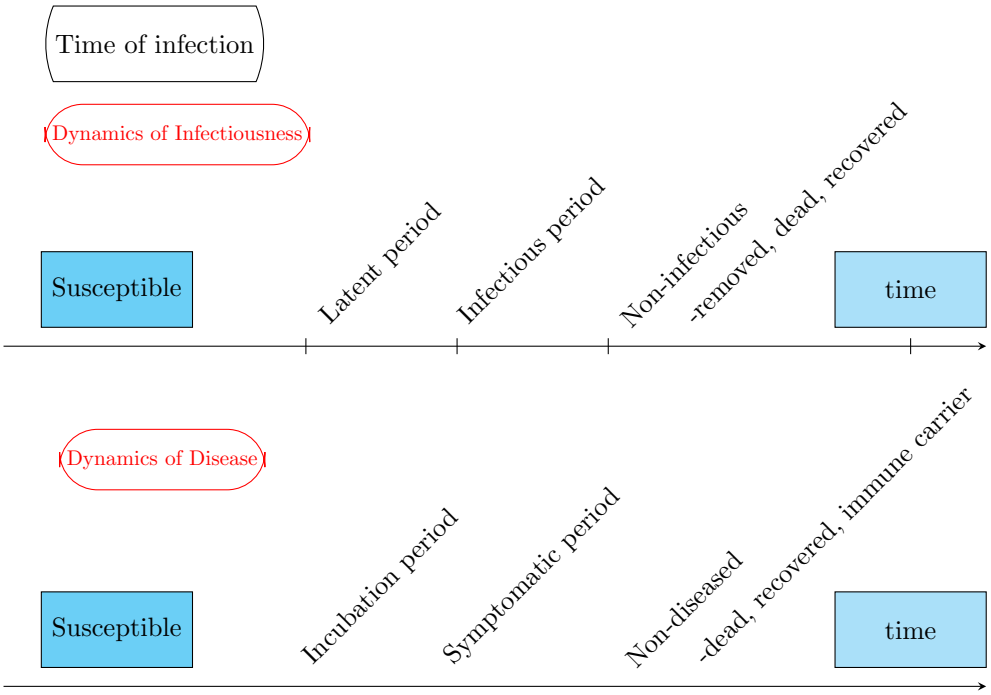

FIGURE 4. Timeline for infection and disease.

One group is asymptomatic and the other is symptomatic, both of which can transmit the disease to healthy people, and in this case, the infected people either recover or die. Therefore, one of the above models can be selected for research. On the other hand, since vaccine administration is one of the effective methods of preventing and reducing viral infections and accurate information is not available from groups such as the number of admissions, etc., we used a simple model called `SEIR` and looked at how well a vaccine would work to predict what might happen with COVID-19 in the future. The system of ordinary differential equations related to the `SEIR` model for COVID-19 in Figure 1 as

follows:

$$\begin{cases} \frac{\mathrm{dS}}{\mathrm{dt}} = -(\nu p_s + d_0)S - \beta(1-\nu p_s)\mathtt{SI} + b_0, \\ \frac{\mathrm{dE}}{\mathrm{dt}} = \beta(1-\nu p_s)\mathtt{SI} - (d_1 + \alpha + (1-\alpha)\nu p_e)\mathtt{E}, \\ \frac{\mathrm{dI}}{\mathrm{dt}} = \alpha\mathtt{E} - (d_2 + \gamma + (1-\gamma)\nu p_i)\mathtt{I}, \\ \frac{\mathrm{dR}}{\mathrm{dt}} = \nu p_s\mathtt{S} + \nu p_e(1-\alpha)\mathtt{E} + (\gamma + (1-\gamma)\nu p_i)\mathtt{I} - d_0\mathtt{R}, \end{cases}$$

via initial conditions $0 \leq \mathtt{S}(0), \mathtt{E}(0), \mathtt{I}(0), \mathtt{R}(0) < 1$.

In this section, we aimed to change the time derivative with the CFD. The ordinary derivative includes an inverse second dimension $\frac{1}{s}$ and the fractional derivative $\mathscr{D}^{\nu}$ has a dimension of $s^{-\nu}$. To solve this problem, we employed an auxiliary parameter θ with a second dimension s called the cosmic time (https://www.worldometers.info/coronavirus).

By the parameter, from a physical point of view, we will have

$$\left[\theta^{\nu-1C}\mathscr{D}^{\nu}\right] = \left[\frac{\mathrm{d}}{\mathrm{dt}}\right] = \frac{1}{s}.$$

Therefore, the COVID-19 mathematical model based on fractional derivatives for $\mathfrak{t} > 0$ and $\lambda \in (0,1)$ is presented as follows:

$$\begin{cases} \theta^{\lambda-1}\mathscr{D}_*^{\lambda}\mathtt{S}(\mathfrak{t}) = -(\nu p_s + d_0)\mathtt{S} - \beta(1-\nu p_s)\mathtt{SI} + b_0, \\ \theta^{\lambda-1}\mathscr{D}_*^{\lambda}\mathtt{E}(\mathfrak{t}) = \beta(1-\nu p_s)\mathtt{SI} - (d_1 + \alpha + (1-\alpha)\nu p_e)\mathtt{E}, \\ \theta^{\lambda-1}\mathscr{D}_*^{\lambda}\mathtt{I}(\mathfrak{t}) = \alpha\mathtt{E} - (d_2 + \gamma + (1-\gamma)\nu p_i)\mathtt{I}, \\ \theta^{\lambda-1}\mathscr{D}_*^{\lambda}\mathtt{R}(\mathfrak{t}) = \nu p_s\mathtt{S} + \nu p_e(1-\alpha)\mathtt{E} + (\gamma + (1-\gamma)\nu p_i)\mathtt{I} - d_0\mathtt{R}, \end{cases} \tag{3.1}$$

such that the initial conditions are

$$\mathtt{S}(0) = \mathtt{S}_0 > 0, \quad \mathtt{E}(0) = \mathtt{E}_0 > 0, \quad \mathtt{I}(0) = \mathtt{I}_0 > 0, \quad \mathtt{R}(0) = \mathtt{R}_0 \geq 0.$$

The variables and parameters used in (3.1) is explained in Table 1.

TABLE 1. The parameters description used in model.

The physical interpretation	Variable/Parameter
Changing rate from E to I	α
Effective transmission rate of COVID-19	β
Changing rate from I to R	γ
Vaccination rate of population	ν
Birth rate of population	b_0
Death rate of population without COVID-19	d_0
Death rates of exposed and infectious population plus d_0	d_1, d_2
Effectiveness of vaccination in E, I, S	p_e, p_i, p_s

Consider the set

$$\Lambda = \left\{(\mathtt{S},\mathtt{E},\mathtt{I},\mathtt{R}) \in C\left([0,\infty)^4\right) \,:\, Y(\mathfrak{t}) \leq \frac{b_0}{d_0}\right\},$$

with $Y = \mathtt{S} + \mathtt{E} + \mathtt{I} + \mathtt{R}$. The next Lemma shows that the closed set Λ is the invariant set with respect to fractional system of (3.1).

Lemma 3.1. *The closed set Λ is positively invariant with respect to fractional system (3.1).*

Proof. By adding all of the relations in system (3.1), we have:

$$\theta^{\lambda-1}(\mathscr{D}_*^{\lambda}\mathtt{S}(\mathtt{t})+\mathscr{D}_*^{\lambda}\mathtt{E}(\mathtt{t})+\mathscr{D}_*^{\lambda}\mathtt{I}(\mathtt{t})+\mathscr{D}_*^{\lambda}\mathtt{R}(\mathtt{t}))=b_0-d_0(\mathtt{S}+\mathtt{E}+\mathtt{I}+\mathtt{R})+(d_0-d_1)+(d_0-d_2)\mathtt{I}.$$

Hence, $\theta^{\lambda-1}\mathscr{D}_*^{\lambda}Y(\mathtt{t})=b_0-d_0(Y(\mathtt{t}))+(d_0-d_1)\mathtt{E}+(d_0-d_2)\mathtt{I}$. Thus,

$$\theta^{\lambda-1}\left(\mathscr{D}_*^{\lambda}Y(\mathtt{t})\right)\leq b_0-d_0Y(\mathtt{t})\Longrightarrow\mathscr{D}_*^{\lambda}Y(\mathtt{t})\leq\theta^{1-\lambda}b_0-\theta^{1-\lambda}d_0Y(\mathtt{t}).$$

By applying [8, Theoremm 7.2] and [8, Remark 7.1], we conclude:

$$Y(\mathtt{t})\leq Y(0)\mathtt{E}_{\lambda}\left(-d_0\theta^{1-\lambda}\mathtt{t}^{\lambda}\right)+\int_0^{\mathtt{t}}b_0\theta^{1-\lambda}z^{\lambda-1}\mathtt{E}_{\lambda,\lambda}\left(-d_0\theta^{1-\lambda}z^{\lambda}\right)\,\mathrm{d}z.$$

Hence,

$$\begin{aligned}
Y(\mathtt{t}) &\leq Y(0)\mathtt{E}_{\lambda}(-d_0\theta^{1-\lambda}\mathtt{t}^{\lambda})+\int_0^{\mathtt{t}}b_0\theta^{1-\lambda}z^{\lambda-1}\sum_{i=0}^{\infty}\frac{(-1)^i d_0^i\theta^{(1-\lambda)i}z^{i\lambda}}{\Gamma(i\lambda+\lambda)}\\
&= Y(0)\mathtt{E}_{\lambda}(-d_0\theta^{1-\lambda}\mathtt{t}^{\lambda})+b_0\theta^{1-\lambda}\sum_{i=0}^{\infty}\frac{(-1)^i d_0^i\theta^{(1-\lambda)i}\mathtt{t}^{i\lambda+\lambda}}{\Gamma(i\lambda+\lambda+1)}\,\mathrm{d}z\\
&= Y(0)\mathtt{E}_{\lambda}(-d_0\theta^{1-\lambda}\mathtt{t}^{\lambda})-\frac{b_0}{d_0}\sum_{i=0}^{\infty}\frac{(-1)^i d_0^i\theta^{(1-\lambda)i}\mathtt{t}^{i\lambda}}{\Gamma(i\lambda+1)}\\
&= Y(0)\mathtt{E}_{\lambda}(-d_0\theta^{1-\lambda}\mathtt{t}^{\lambda})-\frac{b_0}{d_0}(\mathtt{E}_{\lambda}\left(-d_0\theta^{1-\lambda}\mathtt{t}^{\lambda-1}\right))\\
&= \frac{b_0}{d_0}+\mathtt{E}_{\lambda}(-d_0\theta^{1-\lambda}\mathtt{t}^{\lambda})\left(Y(0)-\frac{b_0}{d_0}\right).
\end{aligned}$$

Thus if $Y(0)\leq\frac{1}{d_0}b_0$, then so $Y(\mathtt{t})\leq\frac{1}{d_0}b_0$, for each positive real number $\mathtt{t}$. Therefore, the closed set Λ is positively invariant with respect to fractional model (3.1). This complete the proof. □

4. Equilibrium points and their stability

Equilibrium points of the system (3.1) can be determined by solving the following equations:

$$\mathscr{D}_*^{\lambda}\mathtt{S}(\mathtt{t})=\mathscr{D}_*^{\lambda}\mathtt{E}(\mathtt{t})=\mathscr{D}_*^{\lambda}\mathtt{I}(\mathtt{t})=\mathscr{D}_*^{\lambda}\mathtt{R}(\mathtt{t})=0.$$

That equivalence to

$$\begin{cases}
-(\nu p_s+d_0)\mathtt{S}-\beta(1-\nu p_s)\mathtt{SI}+b_0=0,\\
\beta(1-\nu p_s)\mathtt{SI}-(d_1+\alpha+(1-\alpha)\nu p_e)\mathtt{E}=0,\\
\alpha\mathtt{E}-(d_2+\gamma+(1-\gamma)\nu p_i)\mathtt{I}=0,\\
\nu p_s\mathtt{S}+\nu p_e(1-\alpha)\mathtt{E}+(\gamma+(1-\gamma)\nu p_i)\mathtt{I}-d_0\mathtt{R}=0.
\end{cases}\tag{4.1}$$

It is clearly, whenever there is no spread of the disease; i.e., $\mathtt{E}\equiv 0\equiv\mathtt{I}$, then a disease-free equilibrium (DFE) is occurred. Hence the DFE point is obtained as

$$\varphi_0=(\mathtt{S}_0,\ \mathtt{E}_0,\ \mathtt{I}_0,\ \mathtt{R}_0)=\left(\frac{b_0}{\nu P_s+d_0},\ 0,\ 0,\ \frac{b_0\nu P_s}{d_0(\nu P_s+d_0)}\right).$$

If $\mathtt{R}_0 > 1$, one can find others equilibrium points of the model by solving 4.1. So, we obtain the endemic equilibrium points of the model whenever $\mathtt{S}$, $\mathtt{E}$, $\mathtt{I}$, $\mathtt{R}$ is against zero, and it is in the form: $\varphi_1 = (\mathtt{S}_1, \mathtt{E}_1, \mathtt{I}_1, \mathtt{R}_1)$, where

$$\mathtt{S}_1 = \frac{\xi\eta}{\alpha\beta(1-\nu p_s)}, \quad \mathtt{E}_1 = \frac{b_0}{\xi} - \frac{\eta(\nu p_s + d_0)}{\alpha\beta(1-\nu p_s)}, \quad \mathtt{I}_1 = \frac{\alpha b_0}{\xi\eta} - \frac{(\nu P_s + d_0)}{\beta(1-\nu p_s)},$$
$$\mathtt{R}_1 = \frac{1}{d_0}\left[\frac{\xi\eta\nu p_s}{\alpha\beta(1-\nu p_s)} + \nu p_e(1-\alpha)\left(\frac{b_0}{\xi} - \frac{\eta(\nu p_s + d_0)}{\alpha\beta(1-\nu p_s)}\right) + (\gamma + (1-\gamma)\nu p_i)\left(\frac{\alpha b_0}{\xi\eta} - \frac{1}{\beta(1-\nu p_s)}(\nu p_s + d_0)\right)\right],$$

here $\xi = d_1 + \alpha + (1-\alpha)\nu p_e$, and $\eta = d_2 + \gamma + (1-\gamma)\nu p_i$. Also, $\mathtt{R}_0$ is the basic reproduction number, which is obtained as the spectral radius of FV^{-1} which is equal to spectral radius of $V^{-1}F$ and

$$F = \begin{bmatrix} 0 & \beta(1-\nu p_s)\mathtt{S} \\ \alpha & 0 \end{bmatrix}, \qquad V = \begin{bmatrix} \xi & 0 \\ 0 & \eta \end{bmatrix}. \tag{4.2}$$

It's clearly

$$V^{-1}F = \frac{1}{\xi\eta}\begin{bmatrix} 0 & \beta\eta(1-\nu p_s)\mathtt{S} \\ \alpha\xi & 0 \end{bmatrix}. \tag{4.3}$$

Thus, R_0, corresponding to the DFE, i.e., for $\mathtt{S}(0) = \frac{1}{\nu P_s + d_0} b_0$, is in the form

$$\mathtt{R}_0 = \left[\frac{\alpha\beta(1-\nu p_s)b_0}{\xi\eta(p_s\nu + d_0)}\right]^{0.5}.$$

Theorem 4.1. (i) *The DFE point φ_0 of system (3.1) is globally asymptotic stable;* ii) *The equilibrium point φ_1 of system (3.1) is locally asymptotic stable.*

Proof. The system (3.1) has the jacobian matrix as follows

$$J = \theta^{1-\lambda}\begin{bmatrix} -(\nu p_s + d_0) - \beta(1-\nu p_s)\mathtt{I} & 0 & -\beta(1-\nu p_s)\mathtt{S} & 0 \\ \beta(1-\nu p_s)\mathtt{I} & -\xi & \beta(1-\nu p_s)S & 0 \\ 0 & \alpha & -\eta & 0 \\ \nu p_s & \nu p_e(1-\alpha) & (\gamma + (1-\gamma)\nu p_i) & -d_0 \end{bmatrix}. \tag{4.4}$$

Thus, at $\mathtt{E}(0) = \mathtt{I}(0) = 0$, the Jacobian matrix os system is □

$$J(\mathtt{E}_0) = \theta^{1-\lambda}\begin{bmatrix} -(\nu p_s + d_0) & 0 & -\frac{\beta b_0(1-\nu p_s)}{\nu p_s + d_0} & 0 \\ 0 & -\xi & \frac{\beta b_0(1-\nu p_s)}{\nu p_s + d_0} & 0 \\ 0 & \alpha & -\eta & 0 \\ \nu p_s & \nu p_e(1-\alpha) & \eta - d_2 & -d_0 \end{bmatrix}. \tag{4.5}$$

Now, the characteristic equation of the Jacobian matrix at the DFE point $J(\mathtt{E}_0)$ is

$$\det(J(\mathtt{E}_0) - x\mathtt{I}) = 0.$$

By compute of characteristic polynomial, we obtain:

$$\det(J(\mathtt{E}_0) - x\mathtt{I}) = \theta^{1-\lambda}(x + d_0)(x + \nu p_s + d_0)\Big[x^2 + (\xi + \eta)x + \eta(\alpha + \xi)\Big] = 0. \tag{4.6}$$

The eigenvalues of the characteristic equation are $x = -d_0$, $x = -(d_0 + \nu P_s)$, and the roots of the equation

$$x^2 + (\xi + \eta)x + \eta(\alpha + \xi) = 0.$$

But this equation has two negative real root or no, so $\mathtt{E}_0$ is asymptotically stable in two cases. Now, we consider the Jacobian matrix (3.1) at the endemic equilibrium point $\mathtt{E}_1$.

$$J(\mathtt{E}_1) = \theta^{1-\lambda}\begin{bmatrix} -(\nu p_s + d_0) - \beta(1-\nu p_s)\mathtt{I}_1 & 0 & -\beta(1-\nu p_s)\mathtt{S}_1 & 0 \\ \beta(1-\nu p_s)\mathtt{I}_1 & -\xi & \beta(1-\nu p_s)\mathtt{S}_1 & 0 \\ 0 & \alpha & -\eta & 0 \\ \nu p_s & \nu p_e(1-\alpha) & \eta - d_2 & -d_0 \end{bmatrix}. \tag{4.7}$$

Hence, let

$$\theta^{1-\lambda}\det\begin{bmatrix} -(A+x) & 0 & -\frac{\xi\eta}{\alpha} & 0 \\ A-(d_0+\nu P_s) & -(\xi+x) & \frac{\xi\eta}{\alpha} & 0 \\ 0 & \alpha & -(\eta+x) & 0 \\ \nu P_s & \nu P_e(1-\alpha) & \eta - d_2 & -(d_0+x) \end{bmatrix}$$

$$= -\theta^{1-\lambda}(x+d_0)\det\begin{bmatrix} -(A+x) & 0 & -\frac{\xi\eta}{\alpha} \\ -(x+d_0+\nu P_s) & -(x+\xi) & 0 \\ 0 & \alpha & -(\eta+x) \end{bmatrix}$$

$$= \theta^{1-\lambda}(x+d_0)\Big[x^3 + (A+\xi+\eta)x^2 + (\xi+\eta)Ax + \xi\eta(A-d_0-\nu P_s)\Big],$$

here $A = \frac{1}{\xi\eta}\,\alpha\beta b_0(1-\nu P_s)$. Since $\mathtt{E}_1 > 0$ thus all of real root of characteristic equation are negative and this implies that $\mathtt{E}_1$ is locally asymptotically stable.

5. The model's numerical simulations and interpretation

We simulate model 3.1 under two cases, USA and Iran. The simulation have been done by MATLAB program. The Figure 5 shows that, if the rate of vaccination per day is increased, the infection rate is significantly reduced. Indeed, the vaccination rate has an important role to terminate the pandemic. Hence, the maximum value of $\mathtt{R}_0$ in USA

Table 2. Parameter values and initial populations.

Initial/Parameter	USA	Iran
$\mathtt{S}(0)$	89838×10^{-5}	96689×10^{-5}
$\mathtt{E}(0) + \mathtt{I}(0)$	2177×10^{-5}	591×10^{-5}
$\mathtt{R}(0)$	7985×10^{-5}	272×10^{-4}
β	462×10^{-3}	233×10^{-3}
α	8696×10^{-5}	8696×10^{-4}
γ	686×10^{-4}	686×10^{-4}
b_0	4.9307×10^{-5}	3.285×10^{-5}
d_0	2.459×10^{-5}	1.330×10^{-5}
d_1	2.675×10^{-5}	1.549×10^{-5}
d_2	2.675×10^{-5}	1.549×10^{-5}

and Iran was 2.9985 and 3.4982, respectively. As the vaccination rate (ν) increased, the values of $\mathtt{R}_0$ decreased with respect to effectiveness of prophylactic (p_s) and therapeutic (p_e, p_i) vaccines, as shown in Figure 5. Also, if the rate of vaccination per day of the populations is under 0.00019, (0.019%), in USA and 0.00014, (0.014%), in Iran, the number of people who can get sick from a disease is still high, even with vaccines. According to Figure 5, the infection rate in

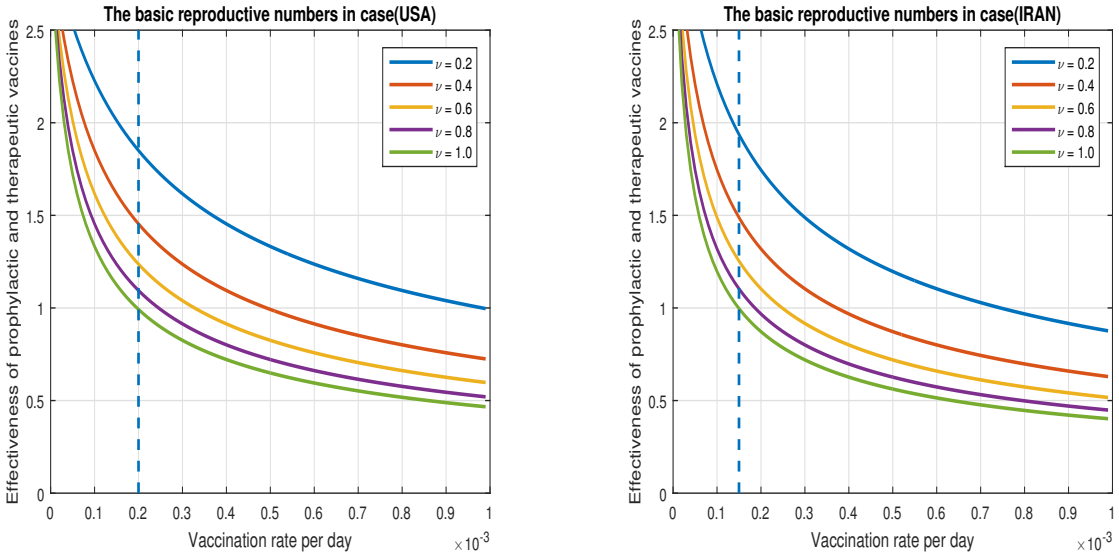

(A) Case USA (B) Case Iran

FIGURE 5. Graphical representation of effectiveness of prophylactic vaccines and treatment for USA and Iran under vaccination rate is $\{0.2, 0.4, 0.6, 0.8, 1.0\}$ with the range of vaccination rate per day.

the two cases USA and Iran will be decreased whenever the rate of vaccination per day is increased $(0-5\%)$ in both countries. Hence the vaccination rate plays an important role to terminate the pandemic. Vaccines can also help reduce the chance of getting sick, for more instance, see https//www.cdc.gov/flu/vaccines-work/vaccineeffect.htm.

Moreover, with the same efficiency of 70% of prophylactic vaccines and 60% of treatment, the USA requires a higher rate of vaccination than Iran to flatten the curve as seen in Figure 6.

Figure 7 depicts the difference between efficiency of prophylactic vaccines and treatment in terms of SARS-CoV-2 infection in humans. The effectiveness of both prophylactic vaccines and treatment was set to the same values. The results demonstrated that prophylactic vaccine had was more efficient than treatment in both the USA and Iran. Prophylactic vaccine can stimulate the immune system and produce long-lived memory lymphocytes [26]. Subsequently, the immune system can rapidly respond to viral infection, resulting in a decrease in infected cases. The equilibrium point related to the USA and Iran situations can be computed by using Equation 4.1. With the vaccination rate 0.1% per day of the USA population ($\nu = 0.001$) and 90% efficiency of prophylactic vaccines and treatment, the equilibrium point corresponding to the fixed parameters in Table 2 of the US case is

$$\varphi_0 = (\mathtt{S}_0, \mathtt{E}_0, \mathtt{I}_0, \mathtt{R}_0) = (0.05333,\ 0,\ 0,\ 2.00516).$$

If there is no vaccine, the equilibrium point of the USA case is

$$\varphi_1 = (\mathtt{S}_1, \mathtt{E}_1, \mathtt{I}_1, \mathtt{R}_1) = (0.14858,\ 0.00034,\ 0.00043,\ 1.18655),$$

that's the illness will not kick the bucket out in the long run. Within the long term, there are almost 0.043% infectious of the USA population. Iran's case has

$$\varphi_0 = (\mathtt{S}_0, \mathtt{E}_0, \mathtt{I}_0, \mathtt{R}_0) = (0.03553,\ 0,\ 0,\ 2.40421),$$

TABLE 3. Numerical values of Effectiveness of prophylactic and therapeutic vaccines.

P_s	$\nu = 0.2$	$\nu = 0.4$	$\nu = 0.6$	$\nu = 0.8$	$\nu = 1.0$
	Case USA				
$0.0E+00$	2.99851	2.99851	2.99851	2.99851	2.99851
$1.0E-05$	2.88353	2.78084	2.68840	2.60460	2.52817
$2.0E-05$	2.78084	2.60460	2.45811	2.33384	2.22670
$3.0E-05$	2.68840	2.45811	2.27838	2.13307	2.01243
$4.0E-05$	2.60460	2.33384	2.13307	1.97655	1.85009
$5.0E-05$	2.52817	2.22670	2.01243	1.85009	1.72160
$6.0E-05$	2.45811	2.13307	1.91019	1.74516	1.61663
$7.0E-05$	2.39356	2.05034	1.82209	1.65627	1.52879
$8.0E-05$	2.33384	1.97655	1.74516	1.57971	1.45386
$9.0E-05$	2.27838	1.91019	1.67722	1.51287	1.38897
⋮	⋮	⋮	⋮	⋮	⋮
$9.0E-04$	1.03945	0.75807	0.62561	0.54472	0.48878
$9.1E-04$	1.03440	0.75415	0.62231	0.54181	0.48616
$9.2E-04$	1.02943	0.75030	0.61906	0.53895	0.48357
$9.3E-04$	1.02453	0.74650	0.61586	0.53614	0.48103
$9.4E-04$	1.01970	0.74277	0.61271	0.53337	0.47853
$9.5E-04$	1.01494	0.73908	0.60961	0.53064	0.47607
$9.6E-04$	1.01024	0.73546	0.60655	0.52795	0.47364
$9.7E-04$	1.00560	0.73188	0.60355	0.52530	0.47125
$9.8E-04$	1.00103	0.72836	0.60058	0.52270	0.46890
$9.9E-04$	0.99653	0.72488	0.59766	0.52013	0.46658
	Case Iran				
$0.0E+00$	3.49842	3.49842	3.49842	3.49842	3.49842
$1.0E-05$	3.26112	3.06636	2.90278	2.76287	2.64142
$2.0E-05$	3.06636	2.76287	2.53469	2.35507	2.20891
$3.0E-05$	2.90278	2.53469	2.27848	2.08698	1.93684
$4.0E-05$	2.76287	2.35507	2.08698	1.89356	1.74556
$5.0E-05$	2.64142	2.20891	1.93684	1.74556	1.60165
$6.0E-05$	2.53469	2.08698	1.81505	1.62759	1.48832
$7.0E-05$	2.43993	1.98323	1.71368	1.53070	1.39608
$8.0E-05$	2.35507	1.89356	1.62759	1.44928	1.31910
$9.0E-05$	2.27848	1.81505	1.55330	1.37961	1.25360
$1.0E-04$	2.20891	1.74556	1.48832	1.31910	1.19697
$1.1E-04$	2.14535	1.68348	1.43088	1.26592	1.14739
$1.2E-04$	2.08698	1.62759	1.37961	1.21869	1.10349
$1.3E-04$	2.03312	1.57692	1.33348	1.17638	1.06427
⋮	⋮	⋮	⋮	⋮	⋮
$9.0E-04$	0.91629	0.65927	0.54145	0.47028	0.42136
$9.1E-04$	0.91159	0.65576	0.53854	0.46774	0.41907
$9.2E-04$	0.90695	0.65231	0.53567	0.46523	0.41681
$9.3E-04$	0.90239	0.64891	0.53285	0.46276	0.41460
$9.4E-04$	0.89789	0.64557	0.53007	0.46034	0.41241
$9.5E-04$	0.89346	0.64228	0.52734	0.45795	0.41027
$9.6E-04$	0.88910	0.63903	0.52465	0.45560	0.40815
$9.7E-04$	0.88480	0.63584	0.52199	0.45328	0.40607
$9.8E-04$	0.88056	0.63269	0.51938	0.45100	0.40402
$9.9E-04$	0.87638	0.62959	0.51681	0.44875	0.40200

for $\nu = 0.001$ and 90% vaccines efficiency, and it has

$$\varphi_1 = (\mathtt{S}_1, \mathtt{E}_1, \mathtt{I}_1, \mathtt{R}_1) = (0.29520, 0.00020, 0.00025, 3.30911),$$

for no vaccines. Similarly to the USA, a few percentages (0.025%) of Iran's populace are irresistible within the long term in case there's no immunization.

Finally, the numerical simulations with different values of CF$\mathbb{D}$ λ are carried out. In Figure 6, we have platted the result of model 3.1 for value $\lambda = 0.97$ and $\nu = 0.001, 0.01, 0.05$. But in Figure 8, the value $\nu = 0.01$ is fixed and the values of λ are 0.80, 0.85, 0.90, 0.95. These results are obtained from Algorithm 1 that are available in the supplementary material section. As you can see in these Figures, The factors have diverse comes about in several sums of λ but show the same behavior. The figure of the USA case appears that the number of individuals with COVID-19

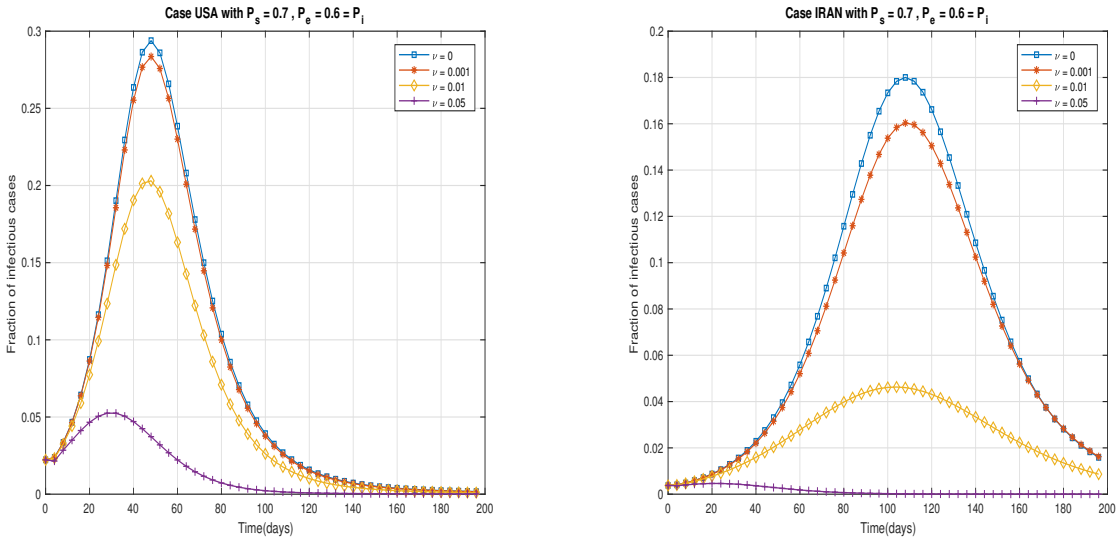

(A) Case USA (B) Case Iran

FIGURE 6. Graphical representation of fraction of USA and Iran infection cases over time if we had 70% effectiveness of prophylactic vaccines and 60% effectiveness of treatment, with different rate of vaccination $\nu = 0, 0.001, 0.01, 0.05\%$ per day of each population.

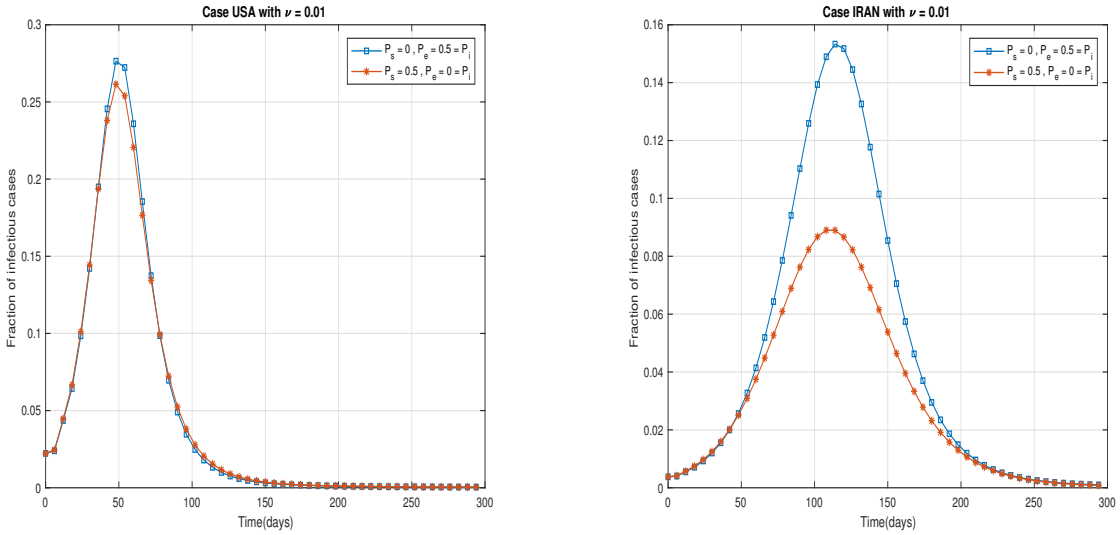

(A) Case USA (B) Case Iran

FIGURE 7. Graphical representation of fraction of USA and Iran infection cases over time if we had 70% effectiveness of prophylactic vaccines and 60% effectiveness of treatment, with different rate of vaccination $\nu = 0, 0.001, 0.01, 0.05\%$ per day of each population

increments until nearly 100 days and after that decreases, but the bend within the Iran case increases until nearly for more than 100 days and after that diminishes. Of course, for less than many infected people.

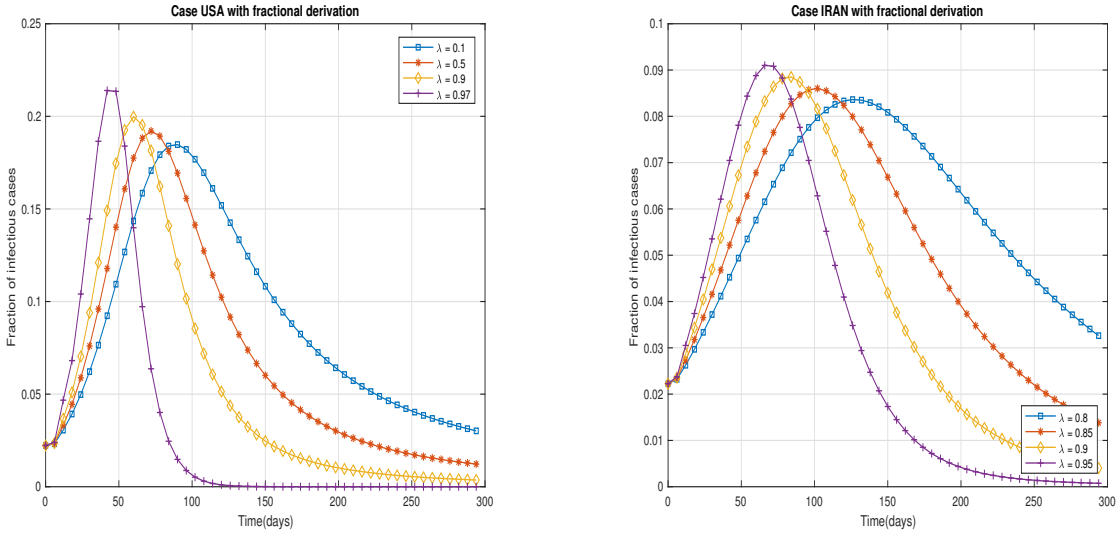

(A) Case USA (B) Case Iran

FIGURE 8. A picture showing how many people in the USA and Iran got sick over time if a vaccine worked really well, preventing 70% of infections of prophylactic vaccines, 60% effectiveness of treatment and rate of vaccination $\nu = 0.01$, with fractional derivative of order $\lambda = 0.80, 0.85, 0.90, 0.95$ per day of each population

Moreover, we have assessed the impacts of fragmentary arrange λ on the dynamical behavior of the Caputo model 3.1 for all three compartments in Iran. As seen in Figure 9a, the vulnerable populace diminished with expanding λ, while as appeared in Figure 9b, with expanding the irresistible populace values of λ expanded, and this makes sense since the helpless populace, after being tainted, is moved to (I) compartment, subsequently coming about in an increment in that. As appeared in Figure 9c, the recouped populace moves forward on the off chance that λ gets huge.

6. Conclusion

We made a model for COVID-19 called `SEIR` and looked at important things like how many people get vaccinated and how well vaccines work to prevent or treat the disease. We found out how fast the system reproduces and where it stops growing. We also studied how steady the system is in a special type of math problem. The number of times a virus can be spread and the points where it stops spreading have been figured out using computer calculations. Our findings show that the system is balanced and steady if each function reaches its equilibrium point.

- The USA situation showed that if 0.1% of people got vaccinated each day and the vaccines were at least 20% effective, the number of people who caught the virus went down. Before vaccines, each person with the virus could spread it to almost 3 other people. But with vaccines, less than 1 person could get it from each sick person.
- Iran had a maximum reproductive number of 3.38, which is the same as the result found.

To obtain the same infection level in both countries, the simulation results revealed that with the same vaccine's efficiency the US would require a higher vaccination rate per day.

Although the research on COVID-19 has been continuously going on and achieved excessive progress, certain limitations, especially in accessing the data source for pandemic modeling, is inevitable. Even when the data is accessible, there is no certainty that the data is complete, or in perfect condition, with full information available. As

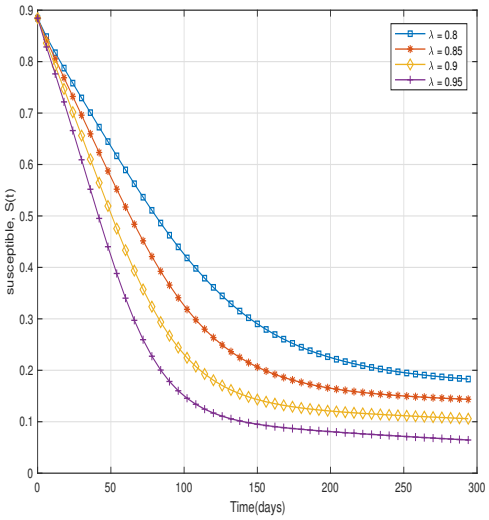

(A) Behavior of the susceptible population for different values of the λ

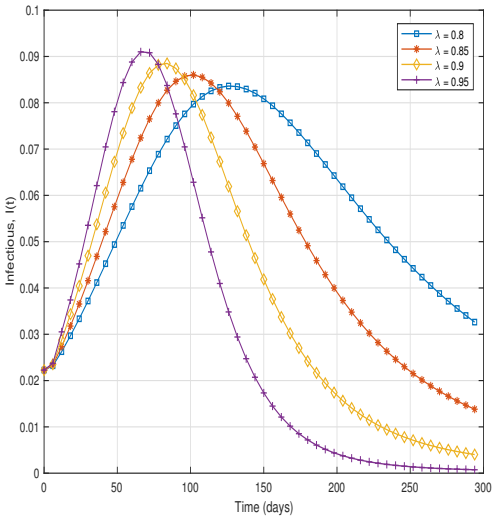

(B) Behavior of the infectious population for different values of the λ

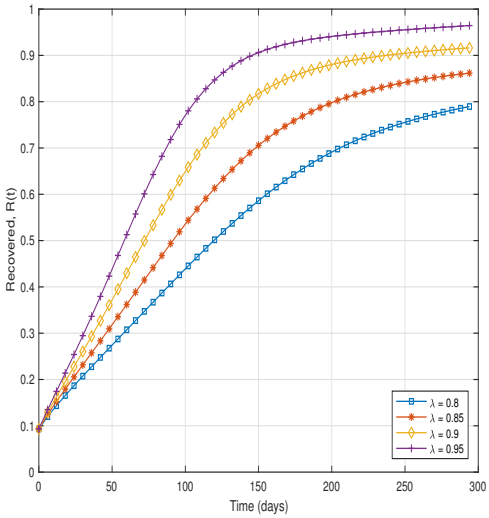

(C) Behavior of the recovered population for different values of the λ

FIGURE 9. Graphical representation of effects of fractional order λ on the dynamical behavior of Caputo model for all three compartments of Iran case per day of each population

a result, despite currently having very few applications to mathematical modeling or pandemic prediction, the Grey Systems theory has tremendous potential for later development. Not only can it make accurate and reliable predictions for policy-making and controlling purposes, but Grey data analysis can also shed light on important insights that can

help us understand much more about the pandemic in the near future, assisting researchers in containing this disease, at the worldwide level.

Therefore, it is recommended that the effect of each of the coefficients in the model on the disease transmission process be evaluated in future studies. Also, more studies are needed to be conducted in order to optimally control the disease spread model and investigate the effect of drugs and vaccination on the current model.

Acknowledgment

This study was approved by institutional review board of Hamadan University of Medical Science (IR. UMSHA. REC. 1401. 084). J. Alzabut is thankful to Prince Sultan University and OSTİM Technical University for their endless support for writing this paper.

References

[1] P. Agarwal, J. J. Nieto, M. Ruzhansky, and D. F. M. Torres, *Analysis of Infectious Disease Problems (COVID-19) and Their Global Impact*, Queen Mary University of London, London, UK, 2021.

[2] F. Ahmed, N. Ahmed, C. Pissarides, and J. Stiglitz, *Why inequality could spread COVID-19*, The Lancet Regional Health, *5*(5) (2020), E240.

[3] M. Altaf Khan and A. Atangana, *Modeling the dynamics of novel coronavirus (2019-nCov) with fractional derivative*, Alexandria Engineering Journal, *59*(4) (2020), 2379–2389.

[4] M. Amdouni, J. Alzabut, M. E. Samei, W. Sudsutad, and C. Thaiprayoon, *A generalized approach of the Gilpin-Ayala model with fractional derivatives under numerical simulation*, Mathematics, *10*(19) (2022), 3655.

[5] S. M. Aydogan, D. Baleanu, H. Mohammadi, and S. Rezapour, *On the mathematical model of Rabies by using the fractional Caputo-Fabrizio derivative*, Advances in Difference Equations, *2020* (2020), 382.

[6] I. A. Baba, U. W. Humphries, F. A. Rihan, and J. E. Nápoles Valdés, *Fractional–order modeling and control of COVID-19 with shedding effect*, Axioms, *12* (2023), 321.

[7] M. Caputo and M. Fabrizio, *A new definition of fractional derivative without singular kernel*, Progress in Fractional Differentiation and Application, *1*(2) (2015), 73–85.

[8] K. Diethelm, *The Analysis of Fractional Differential Equations*, Springer, Berlin, Heidelberg, 2010.

[9] E. F. Doungmo Goufo, *Chaotic processes using the two-parameter derivative with non-singular and non-local kernel: Basic theory and applications*, Chaos, *26*(8) (2016), 084305.

[10] E. F. Doungmo Goufo and A. Atangana, *Analytical and numerical schemes for a derivative with filtering property and no singular kernel with applications to diffusion*, The European Physical Journal Plus, *131* (2016), 269.

[11] A. K. Golmankhaneh, I. Tejado, H. Sevli, and J. E. Nápoles Valdés, *On initial value problems of fractal delay equations*, Applied Mathematics and Computation, *449* (2023), 127980.

[12] T. Guo, Q. Shen, W. Guo, W. He, J. Li, Y. Zhang, Y. Wang, Z. Zhou, D. Deng, X. Ouyang, Z. Xiang, W. Jiang, H. Luo, P. Chen, and H. Peng, *Clinical characteristics of Elderly patients with COVID-19 in Hunan province, China: a multicenter, retrospective study*, Gerontology, *66*(5) (2020), 467–475.

[13] Z. Hu, C. Song, C. Xu, G. Jin, Y. Chen, X. Xu, H. Ma, W. Chen, Y. Lin, Y. Zheng, J. Wang, Z. Hu, Y. Yi, and H. Shen, *Clinical characteristics of 24 asymptomatic infections with COVID-19 screened among close contacts in Nanjing, China*, Sci. China Life Sci., *63*(5) (2020), 706–711.

[14] C. Huang, Y. Wang, X. Li, L. Ren, J. Zhao, Y. Hu, L. Zhang, G. Fan, J. Xu, X. Gu, Z. Cheng, T. Yu, J. Xia, W. Wu, X. Xie, W. Yin, H. Li, M. Liu, Y. Xiao, H. Gao, L. Guo, J. Xie, G. Wang, R. Jiang, Z. Gao, Q. Jin, J. Wang, and B. Cao, *Clinical features of patients infected with 2019 novel coronavirus in Wuhan, China*, Lancet, *395*(10223) (2020), 497–506.

[15] D. S. Hui, E. I. Azhar, T. A. Madani, F. Ntoumi, R. Kock, O. Dar, G. Ippolito, T. D. Mchugh, Z. A. Memish, C. Drosten, A. Zumla, and E. Petersen, *The continuing 2019-nCoV epidemic threat of novel coronaviruses to global health - The latest 2019 novel coronavirus outbreak in Wuhan, China*, International journal of infectious diseases, *91* (2020), 264–266.

[16] M. Jakovljevic, S. Bjedov, N. Jaksic, and I. Jakovljevic, *COVID-19 pandemia and public and global mental health from the perspective of global health securit*, Psychiatr Danub, *32*(1) (2020), 6–14.

[17] M. K. A. Kaabar, V. Kalvandi, N. Eghbali, M. E. Samei, Z. Siri, and F. Martínez, *Generalized Mittag-Leffler-Hyers-Ulam stability of a quadratic fractional integral equation*, Nonlinear Engineering, *10* (2021), 414–427.
[18] A. A. Kilbas, H. M.Srivastava, and J. J. Trujillo, Theory and Applications of Fractional Differential Equations, vol. 204, Elsevier, 2006.
[19] M. Lipsitch, D. L. Swerdlow, and L. Finelli, *Defining the epidemiology of Covid-19 studies needed*, New England journal of medicine, *382*(13) (2020), 1194–1196.
[20] H. Mohammadi, S. Kumar, S. Rezapour, and S. Etemad, *A theoretical study of the Caputo-Fabrizio fractional modeling for hearing loss due to Mumps virus with optimal control*, Chaos Solitons & Fractals, *144* (2020), 110668.
[21] H. Nishiura, T. Kobayashi, T. Miyama, A. Suzuki, S. M. Jung, K. Hayashi, R. Kinoshita, Y. Yang, B. Yuan, A. R. Akhmetzhanov, and N. M. Linton, *Estimation of the asymptomatic ratio of novel coronavirus infections (COVID-19)*, International journal of infectious diseases, *94* (2020), 154–155.
[22] R. Qesmi and A. Hammoumi, *Lifting lockdown control measure assessment: From finite to infinite-dimensional epidemic models for COVID-19*, arXiv, *2021* (2021).
[23] S. Rezapour and H. Mohammadi, *A study on the AH1N1/09 influenza transmission model with the fractional Caputo-Fabrizio derivative*, Advances in Difference Equations, *2020* (2020), 488.
[24] S. Rezapour, H. Mohammadi, and M. E. Samei, *SEIR epidemic model for Covid-19 transmission by caputo derivative of fractional order*, Advances in Difference Equations, *2020* (2020), 490.
[25] M. E. Samei, R. Ghaffari, S. W. Yao, M. K. A. Kaabar, F. Martínez, and M. Inc, *Existence of solutions for a singular fractional $q-$differential equations under Riemann–Liouville integral boundary condition*, Symmetry, *13* (2021), 135.
[26] M. Vajdy, *Induction and maintenance of long-term immunological memory following infection or vaccination*, Frontiers in immunology, *10* (2019), 2658.
[27] D. Wang, B. Hu, C. Hu, F. Zhu, X. Liu, J. Zhang, B. Wang, H. Xiang, Z. Cheng, Y. Xiong, Y. Zhao, Y. Li, X. Wang, and Z. Peng, *Clinical characteristics of 138 hospitalized patients with 2019 novel coronavirus–infected pneumonia in wuhan, china*, JAMA Network, *323*(11) (2020), 1061–1069.
[28] X. Wang, A. Berhail, N. Tabouche, M. M. Matar, M. E. Samei, M. K. A. Kaabar, and X. G. Yue, *A novel investigation of non-periodic snap bvp in the $\mathbb{G}$-caputo sense*, Axioms, *11* (2022) , 390.
[29] P. Wintachai and K. Prathom, *Stability analysis of SEIR model related to efficiency of vaccines for Covid-19 situation*, Heliyon, *7*(4) (2021) , e06812.
[30] H. Zhou, J. Alzabut, S. Rezapour, M. E. Samei, *Uniform persistence and almost periodic solutions of a nonautonomous patch occupancy model*, Advances in Difference Equations, *2020* (2020), 143.
[31] N. Zhu, D. Zhang, W. Wang, X. Li, B. Yang, J. Song, X. Zhao, B. Huang, W. Shi, R. Lu, P. Niu, F. Zhan, X. Ma, D. Wang, W. Xu, G. Wu, G. F. Gao, and W. Tan, *A novel coronavirus from patients with pneumonia in China 2019*, New England Journal of Medicine, *382*(8) (2020), 727–733.